



Contents lists available at SciVerse ScienceDirect

Journal of Sound and Vibration

journal homepage: www.elsevier.com/locate/jsv

Eigenvalue density of linear stochastic dynamical systems: A random matrix approach

S. Adhikari ^{a,*}, L. Pastur ^b, A. Lytova ^b, J. Du Bois ^c^a College of Engineering, Swansea University, Singleton Park, Swansea SA2 8PP, UK^b Department of Theoretical Physics, B.I. Verkin Institute for Low Temperature Physics & Engineering, Kharkov, Ukraine^c Department of Aerospace Engineering, University of Bristol, Bristol BS8 1TR, United Kingdom

ARTICLE INFO

Article history:

Received 28 November 2010

Received in revised form

8 October 2011

Accepted 19 October 2011

Handling Editor: S. Ilanko

Available online 9 November 2011

ABSTRACT

Eigenvalue problems play an important role in the dynamic analysis of engineering systems modeled using the theory of linear structural mechanics. When uncertainties are considered, the eigenvalue problem becomes a random eigenvalue problem. In this paper the density of the eigenvalues of a discretized continuous system with uncertainty is discussed by considering the model where the system matrices are the Wishart random matrices. An analytical expression involving the Stieltjes transform is derived for the density of the eigenvalues when the dimension of the corresponding random matrix becomes asymptotically large. The mean matrices and the dispersion parameters associated with the mass and stiffness matrices are necessary to obtain the density of the eigenvalues in the frameworks of the proposed approach. The applicability of a simple eigenvalue density function, known as the Marčenko–Pastur (MP) density, is investigated. The analytical results are demonstrated by numerical examples involving a plate and the tail boom of a helicopter with uncertain properties. The new results are validated using an experiment on a vibrating plate with randomly attached spring–mass oscillators where 100 nominally identical samples are physically created and individually tested within a laboratory framework.

© 2011 Elsevier Ltd. All rights reserved.

1. Introduction

Uncertainties are unavoidable in the description of complex dynamical systems such as helicopters and aircrafts. Within the scope of probabilistic methods, two broad approaches have been adopted in the literature, namely the parametric approach and the non-parametric approach. In the parametric approach, uncertainties in geometric parameters, material properties such as Poisson's ratio, Young's modulus, mass density and damping coefficients are modeled using random variables or random fields. These uncertainties can be systematically propagated using the stochastic finite element method [1,2]. Non-parametric or model uncertainties do not explicitly depend on the system parameters. For example, there can be unquantified errors associated with the equation of motion (linear or nonlinear), in the damping model (viscous or non-viscous), in the model of structural joints. Model uncertainties may be tackled by the so-called non-parametric method such as the random matrix based approach pioneered by Soize [3,4] and subsequently adopted by others [5–8]. The equation of motion of a damped n -degree-of-freedom linear dynamic system can be expressed as

$$\mathbf{M}\ddot{\mathbf{q}}(t) + \mathbf{C}\dot{\mathbf{q}}(t) + \mathbf{K}\mathbf{q}(t) = \mathbf{f}(t), \quad (1)$$

* Corresponding author. Tel.: +44 1792 602969; fax: +44 1792 295676.

E-mail address: S.Adhikari@swansea.ac.uk (S. Adhikari).

where $\mathbf{f}(t) \in \mathbb{R}^n$ is the forcing vector, $\mathbf{q}(t) \in \mathbb{R}^n$ is the response vector and $\mathbf{M} \in \mathbb{R}^{n \times n}$, $\mathbf{C} \in \mathbb{R}^{n \times n}$ and $\mathbf{K} \in \mathbb{R}^{n \times n}$ are the mass, damping and stiffness matrices respectively. In order to completely quantify the uncertainties associated with system (1) we need to have the probability laws of the random matrices \mathbf{M} , \mathbf{C} and \mathbf{K} . Using the parametric approach, such as the stochastic finite element method, one usually obtains a problem specific covariance structure for the elements of system matrices. This can be obtained either by random variables or by discretizing the random fields using the Karhunen–Loève expansion. The non-parametric approach, on the other hand, results in a central Wishart distribution for the system matrices, see e.g. [3,4] for the justification of the use of approach in structural mechanics.

For stochastic structural dynamic problems, the study of random eigenvalues play a crucial role as the dynamic response is governed by the eigenvalues. The undamped eigenvalue problem corresponding to Eq. (1) can be given by

$$\mathbf{K}\phi_j = \omega_j^2 \mathbf{M}\phi_j, \quad j = 1, 2, \dots, n, \quad (2)$$

where ω_j^2 and ϕ_j are respectively the eigenvalues and mass-normalized eigenvectors of the system. The parametric uncertainties and related random eigenvalue problems are considered in a number of papers (see [9–19] and references therein for example). However, for the Wishart random matrix based non-parametric approach, till date only Monte Carlo simulation based methods are used for the eigenvalue problem. Since the Wishart random matrix based method for stochastic structural dynamics is now a well established method, it may be useful to develop understanding on the nature of the eigenvalues for further application of this method.

The aim of this paper is to develop analytical methods for the analysis of the density of the eigenvalues when the system matrices are modeled by Wishart random matrices, in particular, to derive the large size asymptotic form of the density under certain assumptions. This may help further understanding on the Wishart random matrix model for stochastic structural dynamical systems. The outline of the paper is as follows. A brief overview of random matrix models in probabilistic structural dynamics is given in Section 2. The density of the eigenvalues are discussed Section 3. In Sections 4 and 5 the accuracy of the proposed results regarding the density of the eigenvalues are verified numerically and experimentally. Based on the study taken in the paper, a set of conclusions are drawn in Section 6. The details of derivation of results of Section 3 are presented in Appendix A.

2. The Wishart random matrix model

2.1. Background on Wishart distribution

Random matrices were introduced by [20] in the context of multivariate statistics. However, the Random Matrix Theory (RMT) was not used in other branches until 1950s when [21] published his works (leading to the Nobel prize in Physics in 1963) on the eigenvalues of random matrices arising in high-energy physics. Using an asymptotic theory for large dimensional matrices, Wigner was able to bypass the Schrödinger equation and explain the statistics of measured atomic energy levels in terms of the limiting eigenvalues of these random matrices. Since then research on random matrices has continued to attract interests in multivariate statistics, physics, number theory and more recently in mechanical and electrical engineering. We refer the review works [22–31] for the history and applications of random matrix theory.

Among the various random matrix models, Wishart random matrix model is particularly relevant to structural dynamics due to its symmetry and positive-definiteness property. If \mathbf{X} is a $n \times p$ Gaussian random matrix with identical and independent distribution (i.i.d.) entries, then the matrix $\mathbf{S} = \mathbf{X}\mathbf{X}^T$ has the Wishart distribution. The probability density function of a Wishart random matrix can be expressed as

$$p_{\mathbf{S}}(\mathbf{S}) = \left\{ 2^{(1/2)np} \Gamma_n \left(\frac{1}{2} p \right) |\Sigma|^{(1/2)p} \right\}^{-1} |\mathbf{S}|^{(1/2)(p-n-1)} \text{etr} \left\{ -\frac{1}{2} \Sigma^{-1} \mathbf{S} \right\}. \quad (3)$$

This distribution is usually denoted as $\mathbf{S} \sim W_n(p, \Sigma)$. Here p and Σ are respectively the scalar and matrix parameter of the Wishart distribution. For a realistic distribution Σ should be a $n \times n$ positive definite matrix and $p \geq n$. We refer to a recent book [28] for more detailed discussions on the eigenvalues of Wishart random matrices.

2.2. Parameter selection for structural dynamics

We assume that the baseline model of the system under consideration is known. Since the proportional damping model is assumed, the baseline model consists of the mass and the stiffness matrices given by $n \times n$ matrices \mathbf{M}_0 and \mathbf{K}_0 . These matrices are in general large banded matrices and can be obtained using the conventional finite element method [32–35]. In addition to this, it is assumed that the dispersion parameters associated with these matrices are known. The dispersion parameter, proposed by Soize [3,4], is a measure of uncertainty in the system and it is similar to the normalized standard deviation of matrix. For example, the dispersion parameter associated with the mass matrix \mathbf{M} is defined as

$$\delta_M^2 = \frac{\mathbb{E}\{\|\mathbf{M} - \mathbf{M}_0\|_F^2\}}{\|\mathbf{M}_0\|_F^2}, \quad (4)$$

where $\|\cdot\|_F$ denotes the Frobenius (or Hilbert–Schmidt) norm of a matrix, and the symbol $\mathbb{E}\{\dots\}$ denotes the operation of averaging with respect to the corresponding probability distribution. The dispersion parameter δ_K associated with the

stiffness matrix \mathbf{K} can be defined in a similar way. The dispersion parameters δ_M and δ_K can be obtained using the stochastic finite element method [7,8] or experimental measurements [5,36]. Given the dispersion parameters δ_M and δ_K and the baseline mass and stiffness matrices \mathbf{M}_0 and \mathbf{K}_0 , the parameters for the random matrices \mathbf{M} and \mathbf{K} can be obtained in closed form. Various parameter selection options have been investigated and optimal parameters can be obtained via closed form expressions using optimisation approaches [7].

Over the past decade, it has been established in a number of works (see e.g. [3–8]) that one obtains a fairly reasonable model in structural dynamics assuming that the matrices \mathbf{K} and \mathbf{M} are the Wishart matrices, widely known in multivariate analysis and random matrix theory and its applications [23,25–27,29–31,37,38]. An equivalent form of (2) is the standard eigenvalue problem for the matrix

$$\Xi = \mathbf{M}^{-1/2} \mathbf{K} \mathbf{M}^{-1/2}. \tag{5}$$

It turns out that the eigenvalue problem (2) (or (5)) is fairly difficult to solve analytically when both \mathbf{K} and \mathbf{M} are Wishart matrices. Therefore, the possibility of using the single Wishart is investigated here.

Note that if \mathbf{K} and \mathbf{M} are the Wishart matrices, the matrix Ξ is not Wishart (see e.g. [37] for its distribution). Let us consider the simplest case where the mass matrix \mathbf{M} is deterministic. In this case the dynamical matrix Ξ is also a Wishart matrix. In a recent work [8], however, the possibility of Ξ itself being a Wishart matrix for the general case was investigated. Since Ξ is a positive definite matrix, a Wishart can be fitted using the maximum entropy principle or otherwise [7], just like the mass and stiffness matrices provided the dispersion parameter and the baseline value are known. It was observed that such a single Wishart matrix also provides a reasonable model [8]. Thus the proposed approach does not strictly follow from the original Wishart matrix model of the system matrices and should be considered as one used for mathematical simplicity and computational efficiency, providing the qualitative (and in some cases quantitative) description of stochastic dynamics. The detailed derivation of such generalized Wishart matrix and its numerical and experimental validation can be found in Ref. [8].

We consider an equivalent Wishart distribution for the matrix $\Xi \sim W_n(p, \Sigma)$. We refer to the books by Muirhead [26], Girko [25], Gupta and Nagar [37] and Tulino and Verdú [23] for discussions on Wishart random matrices and related mathematical topics. The parameters p and Σ can be obtained from the available data regarding the system, namely \mathbf{M}_0 , \mathbf{K}_0 , δ_M , and δ_K . Following Ref. [8], we have

$$\Xi \sim W_n(p, \Sigma), \tag{6}$$

where

$$\Sigma = \Omega_0^2 / \theta, \quad p = n + 1 + \theta, \quad \text{and} \quad \theta = \frac{(1 + \beta)}{\delta^2} - (n + 1). \tag{7}$$

The matrix Ω_0 is a diagonal matrix containing the undamped natural frequencies of the baseline model ω_{0j} . The constant β and the dispersion parameter δ can be obtained as

$$\beta = \left(\sum_{j=1}^n \omega_{0j}^2 \right)^2 / \sum_{j=1}^n \omega_{0j}^4 \tag{8}$$

and

$$\delta = \frac{(p_1^2 + (p_2 - 2 - 2n)p_1 + (-n - 1)p_2 + n^2 + 1 + 2n)\beta}{p_2(-p_1 + n)(-p_1 + n + 3)} + \frac{p_1^2 + (p_2 - 2n)p_1 + (1 - n)p_2 - 1 + n^2}{p_2(-p_1 + n)(-p_1 + n + 3)}. \tag{9}$$

Here the constants

$$p_1 = \frac{1}{\delta_M^2} \{1 + \{\text{Tr}(\mathbf{M}_0)\}^2 / \text{Tr}(\mathbf{M}_0^2)\} \quad \text{and} \quad p_2 = \frac{1}{\delta_K^2} \{1 + \{\text{Tr}(\mathbf{K}_0)\}^2 / \text{Tr}(\mathbf{K}_0^2)\}. \tag{10}$$

These relationships completely define all the parameters of the Wishart random matrix necessary to study the density of the eigenvalues. Dynamical response obtained using this generalized Wishart matrix has been validated against the stochastic finite element method, full Wishart matrices and experiential results [8]. Here we take this model to study the density of the eigenvalues.

3. Density of the eigenvalues of Wishart matrices

The spectral properties of the Wishart random matrix Ξ play a key role in the uncertainty quantification of stochastic dynamical systems. For low frequency vibration problems and if the size of matrices and/or the amount of uncertainties is not too large, the probability distributions of individual eigenvalues provide a useful physical insight. However, for random systems when the system parameters vary, the eigenvalues may show the veering effect [39,40]. Additionally, for higher eigenvalues of a random system and for sufficiently large matrices and/or the amount of uncertainties, the eigenvalues start to statistically overlap each other [41]. Soize [42] showed that for moderately uncertain system ($\delta_k^2 = 0.25$), there can be significant statistical overlap even for eigenvalue number as low as 30. When there is mode veering and significant

statistical overlap of the eigenvalues, the physical significance of the probability distribution of individual ordered eigenvalues becomes questionable. For instance, the perturbation type approach [43,44] may seem less valid as the standard deviation of the eigenvalues becomes more than the mean spacing between the eigenvalues. In this case an alternative approach which considers the density of a collection of eigenvalues [27] seems more meaningful. This type of approach may be particularly useful for aerospace structures such as helicopters and spacecrafts as they are often subjected to high frequency vibrations which may excite many higher modes. For example, it is estimated that NASA’s Saturn launch vehicle had about 500,000 modes in the range of 0–2 kHz [45].

Motivated by these, we will discuss in this section the density of the eigenvalues of linear dynamical systems modeled by Wishart random matrices. The density is the simplest but quite important characteristic of a random dynamical system, providing primary information on their eigenvalue distribution and determining a number of other properties, in particular, the response statistics. The eigenvalue density of the Gaussian Orthogonal Ensembles (GOE) matrices have been used previously [46,47] to obtain dynamic response of random systems. In the similar way, the results to be derived in this paper could be useful to obtain response statistics when the eigenvalue distribution is modeled using the Wishart random matrix ensemble. In the following subsections, only the main results are described. The detailed derivations are given in Appendix A.

3.1. Linear eigenvalue statistics

In this section linear statistics of eigenvalues are considered. The interest is in the limit when the dimension of the system is very large, that is, $n \rightarrow \infty$. Such large systems are widely used in many high-fidelity numerical models of aerospace and mechanical systems. This is particularly true for vibration problems where a fine mesh size in the finite element model is necessary to capture short wave lengths. We define the density of the random eigenvalues as

$$\rho_n(\lambda) = n^{-1} \sum_{l=1}^n \delta(\lambda - \lambda_l^{(n)}), \tag{11}$$

where

$$\lambda_1^{(n)}, \dots, \lambda_n^{(n)} \tag{12}$$

are the random eigenvalues (natural frequency squared) of the corresponding stochastic dynamical system, and δ is the Dirac delta-function. We intend to find analytical descriptions of the following two moments:

$$(i) \quad \mathbb{E}\{\rho_n(\lambda)\} \quad \text{as } n \rightarrow \infty, \tag{13}$$

$$(ii) \quad \mathbb{E}\{\rho_n^2(\lambda)\} \quad \text{as } n \rightarrow \infty. \tag{14}$$

The problems (13) and (14) are well studied in the random matrix theory and its applications (see e.g. [22–31] and references therein) as well as in the random operator theory (see e.g. [48,49] and references therein). We outline below the results, which are pertinent for the stochastic structural dynamics and to the best of our knowledge has not yet received detailed attention.

Note that while (13) is well defined, this is not the case for (14). Indeed, we have by definition

$$\rho_n^2(\lambda) = n^{-2} \sum_{l_1, l_2=1}^n \delta(\lambda - \lambda_{l_1}^{(n)}) \delta(\lambda - \lambda_{l_2}^{(n)}) = n^{-2} \sum_{l_1=1}^n \delta^2(\lambda - \lambda_{l_1}^{(n)}) + n^{-2} \sum_{l_1 \neq l_2} \delta(\lambda - \lambda_{l_1}^{(n)}) \delta(\lambda - \lambda_{l_2}^{(n)}),$$

and we see that summand $\delta^2(\lambda - \lambda_{l_1}^{(n)})$ of the first sum on the r.h.s. is not well defined (it is often said that the square of delta-function is infinity).

To avoid this we have to “smooth” the delta-function by replacing it with a regular function having a well pronounced peak at zero. If we denote this function u , then we have

$$n^{-1} \sum_{l=1}^n u(\lambda - \lambda_l^{(n)}) = \int u(\lambda - \mu) \rho_n(\mu) \, d\mu \tag{15}$$

instead of ρ_n of (11). The smoothing is unavoidable, in particular, when one computes $\rho_n(\lambda)$ numerically, because one first finds the eigenvalues and then draws a continuous envelope curve which corresponds to smoothing ρ_n with a function u whose peak has a width bigger than the distance (of the order $O(n^{-1})$) between the eigenvalues. This is why we will not deal with ρ_n itself but rather with so-called *normalized linear eigenvalue statistics*, defined for any sufficiently smooth test function φ as

$$N_n[\varphi] := n^{-1} \sum_{l=1}^n \varphi(\lambda_l^{(n)}) = \int \varphi(\mu) \rho_n(\mu) \, d\mu. \tag{16}$$

Note that ρ_n of (11) corresponds formally to $\varphi(\mu) = \delta(\lambda - \mu)$ for a given λ and the smoothed density (15) of ρ_n corresponding to $\varphi(\mu) = u_\lambda(\mu) := u(\lambda - \mu)$. Another motivation to consider linear statistics is that we need quite often not the density ρ_n itself but the integrals of products of ρ_n and certain known function (observables), or, in other words, the sum over the spectrum of certain function of frequency. We consider now the density of eigenvalues within these general frameworks of the random matrix theory.

3.2. The self-averaging property of the eigenvalue density

We start from an appropriate form of problem (14), since it is not only of interest in its own, but also will also be used in solving problem (13). We consider the variance

$$\mathbb{V}\{N_n[\varphi]\} = \mathbb{E}\{|N_n[\varphi]|^2\} - |\mathbb{E}\{N_n[\varphi]\}|^2 \tag{17}$$

of a linear eigenvalue statistic of Wishart matrices. This is the simplest measure of the fluctuations of $N_n[\varphi]$ around its expectation $\mathbb{E}\{N_n[\varphi]\}$. It is shown in Appendix A that $\mathbb{V}\{N_n[\varphi]\}$ vanishes sufficiently fast in the limit

$$n \rightarrow \infty, \quad p \rightarrow \infty, \quad p/n \rightarrow c \in (1, \infty). \tag{18}$$

Namely, we have the bound

$$\mathbb{V}\{N_n[\varphi]\} \leq \frac{4}{\beta n^2 p} \text{Tr } \Sigma^2 \left(\max_{\lambda \in \mathbb{R}} |\varphi'(\lambda)| \right)^2, \tag{19}$$

where $\beta = 1$ for real symmetric and $\beta = 2$ for hermitian Wishart matrices.

It can be shown that if we want to keep the spectrum of Ξ bounded for all n, p of (18) rather than escaping to infinity, we have to assume that in the limit (18)

$$\max_n n^{-1} \text{Tr } \Sigma^2 \leq C < \infty. \tag{20}$$

Similarly, in fact stronger, condition is necessary to find (13). Assuming this and

$$\max_{\lambda \in \mathbb{R}} |\varphi'(\lambda)| < \infty, \tag{21}$$

we obtain from (19) that

$$\mathbb{V}\{N_n[\varphi]\} = O(n^{-2}) \tag{22}$$

under condition (18), (20) and (21).

Note that if the eigenvalues (12) of Ξ were i.i.d. random variables, then the variance of their linear statistics is equal to $n^{-1} \mathbb{V}\{\varphi(\lambda_1)\}$, i.e., is $O(n^{-1})$ for any φ such that $\mathbb{V}\{\varphi(\lambda_1)\} < \infty$ (see (25) and (26)). Thus, (22) is the manifestation of strong statistical dependence between the eigenvalues of Wishart random matrices, known also as the repulsion of eigenvalues and/or the rigidity of spectrum (see e.g. [27]).

It is also worth to emphasize that the order $O(n^{-2})$ in (22) is the case if the test-functions satisfy (21). Consider, for instance, the Heaviside function

$$\varphi_H(\lambda) = \begin{cases} \varphi_0, & \lambda \in [a, b], \\ 0 & \text{otherwise,} \end{cases}$$

as φ in (16). In this case $N_n[\varphi]$ is just the relative number $N_n(a, b)$ of eigenvalues of Ξ falling in the interval $[a, b]$. It can be shown that at least for $\Sigma = a^2 \mathbf{I}_n$ we have

$$\mathbb{V}\{N_n(a, b)\} = \frac{\log n}{\pi^2 n^2} (1 + o(1)), \quad n \rightarrow \infty. \tag{23}$$

Thus the rate of decay of the variance of the normalized linear eigenvalue statistics of Ξ depends on the smoothness of the test function but it is faster than $O(n^{-1})$, i.e., the rate for i.i.d. random variables, for sufficiently large class of continuous test functions [28].

The fact that the fluctuations of linear eigenvalue statistics around their mean are $O(n^{-2})$ as in (22) implies that for large systems the density is effectively deterministic. This property is known as the *self-averaging property* in random matrix theory and the theory of disordered systems (see e.g. [27]). The property is similar to the Law of Large Numbers of probability theory, according to which if $\xi_1, \xi_2, \dots, \xi_n$ are independent identically distributed (i.i.d.) random variables, then the random variable

$$L_n = n^{-1} \sum_{l=1}^n \xi_l \tag{24}$$

tends to the non-random limit $\mathbb{E}\{\xi_1\}$ as $n \rightarrow \infty$. The simplest manifestation of this is the form of variance

$$\mathbb{V}\{L_n\} := \mathbb{E}\{|L_n|^2\} - |\mathbb{E}\{L_n\}|^2 = n^{-1} \mathbb{V}\{\xi_1\} = n^{-1} (\mathbb{E}\{|\xi_1|^2\} - |\mathbb{E}\{\xi_1\}|^2) \tag{25}$$

of L_n . Indeed, it follows from the above that if $\mathbb{E}\{|\xi_1|^2\}$ is finite, then

$$\mathbb{V}\{L_n\} = O(n^{-1}), \quad n \rightarrow \infty, \tag{26}$$

i.e., the fluctuations of L_n are negligible for large n . In Section 4 we demonstrate the self-averaging property using numerical and experimental methods.

3.3. Asymptotic density of the eigenvalues

Let Ξ be an $n \times n$ real symmetric or hermitian Wishart matrix with p degrees of freedom and an $n \times n$ matrix Σ , i.e., $\Xi \sim W_n(p, \Sigma)$ or

$$\Xi = p^{-1} \Sigma^{1/2} \mathbf{X} \mathbf{X}^T \Sigma^{1/2}, \tag{27}$$

here $\mathbf{X} = \{X_{j\alpha}\}_{j,\alpha=1}^{n,p}$ is the $n \times p$ matrix, whose entries are the standard Gaussian random variables, determined by the relations

$$\mathbb{E}\{X_{j\alpha}\} = 0, \quad \mathbb{E}\{X_{j_1\alpha_1} X_{j_2\alpha_2}\} = \delta_{j_1 j_2} \delta_{\alpha_1 \alpha_2}, \tag{28}$$

and Σ is positive definite.

All the parameters of Ξ have been explicitly defined in Section 2 and the model has been numerically and experimentally validated [8]. Consider the linear statistic (16) of eigenvalues of Ξ , corresponding to a real or complex valued test function φ . It can be shown (see [29,50,51] and Appendix A) that

$$\lim_{n \rightarrow \infty, p \rightarrow \infty, p/n \rightarrow c \in [1, \infty)} \mathbb{E}\{N_n[\varphi]\} = \int \varphi(\lambda) \rho(\lambda) d\lambda, \tag{29}$$

where ρ is the limiting eigenvalue density of Ξ that can be found by solving a functional equation for its Stieltjes transform [23]

$$f(z) = \int \frac{\rho(\lambda) d\lambda}{\lambda - z}, \quad \Im z \neq 0. \tag{30}$$

Given f , one can find ρ from the inversion formula

$$\rho(\lambda) = \pi^{-1} \Im f(\lambda + i0). \tag{31}$$

Assuming that the limiting eigenvalue density of Σ exists and denoting it v , we can write the equation for f of (30) as (see Appendix A)

$$f(z) = c \int \frac{v(\sigma) d\sigma}{\sigma((c-1)-zf(z))-cz}. \tag{32}$$

The equation has to be solved in the class of functions, analytic for $\Im z \neq 0$ and such that

$$\Im f(z) \Im z > 0, \quad \Im z \neq 0. \tag{33}$$

Given the eigenvalue density v of Σ which is related to the mean system matrix, Eqs. (32) and (33) give an algorithm to find the density of eigenvalues of the corresponding random system. In Eqs. (32) and (33) the eigenvalue density v of the baseline model can be viewed the “input data” and the Stieltjes transform $f(z)$ of (32), determining the density ρ of the random eigenvalues via (31), can be viewed as the “output data”. In view of the definition of Σ in Eq. (7), one can relate the eigenvalues Σ with the undamped natural frequencies as

$$\{\sigma_1, \sigma_2, \dots, \sigma_n\} = \{\omega_{0_1}^2/\theta, \omega_{0_2}^2/\theta, \dots, \omega_{0_n}^2/\theta\}. \tag{34}$$

The value of θ in Eq. (7) is related to the dispersion parameter of the random matrix. From the values of $\{\sigma_j\}_{j=1}^n$, the input density v can be obtained from their normalized histogram if n is large enough. This in turn implies that v can be obtained from the conventional deterministic finite element approach. Therefore, using this approach, the conventional finite element method can be used to obtain the eigenvalue density of the corresponding random system.

3.4. The Marčenko–Pastur (MP) density

Eqs. (32) and (33) is hard to solve in closed form for an arbitrary v . Numerical methods are normally necessary to solve the equation and obtain the limiting density of the random eigenvalues from (31). We consider the simplest case where the profile of the undamped eigenvalues is asymptotically ‘flat’, hence

$$v(\sigma) = \delta(\sigma - a^2). \tag{35}$$

This is often the case with many systems in the high frequency, for example, the rectangular plate considered in the next section. For this case the matrix Σ becomes the unit matrix times $a^2 > 0$, that is $\Sigma = a^2 \mathbf{I}_n$. Using this, Eq. (32) reduces to the quadratic equation

$$a^2 z f^2(z) + (cz + a^2(1-c))f(z) + c = 0, \tag{36}$$

whose solution, satisfying (33), is

$$f(z) = \frac{-(cz + a^2(1-c)) + \sqrt{(cz + a^2(1-c))^2 - 4a^2cz}}{2a^2z}, \quad (37)$$

where the branch of square root is defined by its asymptotic $cz + O(1)$, $z \rightarrow \infty$.

Substituting $f(z)$ from Eq. (37) into Eq. (31) yields that, for $c > 1$

$$\rho(\lambda) = \frac{c}{2\pi a^2 \lambda} \begin{cases} \sqrt{(a_+ - \lambda)(\lambda - a_-)}, & \lambda \in [a_-, a_+], \\ 0, & \lambda \notin [a_-, a_+], \end{cases} \quad (38)$$

where

$$a_{\pm} = a^2(1 \pm c^{-1/2})^2. \quad (39)$$

For $c=1$ one obtains

$$\rho(\lambda) = \frac{1}{2\pi a^2} \begin{cases} \sqrt{(4a^2 - \lambda)/\lambda}, & \lambda \in (0, 4a^2], \\ 0, & \lambda \notin (0, 4a^2]. \end{cases} \quad (40)$$

The density of eigenvalues given by Eq. (38) or Eq. (40) is now known as Marčenko–Pastur (MP) density [50].

Recall that $c=p/n$ and p given by Eq. (7). Therefore p is always greater than n and we have $c \geq 1$. As a result, the MP density given by Eq. (38) need to be used. The parameters can be obtained by looking at the domain of validity, namely $[a_-, a_+]$. Suppose $\omega_{0_{\min}}$ and $\omega_{0_{\max}}$ are the lowest and the highest natural frequency of the baseline dynamical system under consideration. Since $\lambda_j = \omega_j^2$ we have

$$a_- = \omega_{0_{\min}}^2 \quad \text{and} \quad a_+ = \omega_{0_{\max}}^2. \quad (41)$$

Using these values, and solving the two equations given by (39) one obtains

$$c = \left(\frac{\omega_{0_{\max}} + \omega_{0_{\min}}}{\omega_{0_{\max}} - \omega_{0_{\min}}} \right)^2 \quad \text{and} \quad a = (\omega_{0_{\max}} + \omega_{0_{\min}})/2. \quad (42)$$

Eq. (38), together with (41) and (42) completely defines the MP density for the eigenvalues of a stochastic linear dynamical system. The validity of this density function will be examined in the next section using numerical and experimental studies.

4. Numerical and experiential studies: a rectangular plate with uncertain properties

Given the density of undamped eigenvalues v , we derived in the previous section Eq. (32) for the density of eigenvalues of the corresponding random system (the ‘output density’). The density of undamped eigenvalues (the ‘input density’) can be obtained using the finite element method together with the dispersion parameter. In general numerical methods are necessary to solve Eq. (32). Since the equation is in terms of the Stieltjes transform, an explicit form of the output density is not easy to find. This is why a simple formula (38) was derived for a special case where the input density is (35). It was also proved that for large random dynamical systems, the density of eigenvalues of the random system reaches a non-random limit. In this section we examine the validity of these results using numerical examples and an experimental study. We also verify if the MP density (40) is valid for structural dynamic systems. The analytical results derived in the previous section is based on asymptotic theory, that is, when n is infinitely large. On the contrary, the numerical examples considered here are for finite values of n .

A rectangular cantilever steel plate is considered to illustrate the convergence of the eigenvalue-density. The deterministic properties are assumed to be $\bar{E} = 200 \times 10^9$ N/m², $\bar{\mu} = 0.3$, $\bar{m} = 7860$ kg/m³, $\bar{t} = 3.0$ mm, $L_x = 0.998$ m, $L_y = 0.59$ m. The discretized model has 4650 degrees-of-freedom. The Wishart random matrix model given by Eq. (6) has a parameter matrix which is a general diagonal matrix. The density of eigenvalues of such matrices cannot be obtained by closed-form expression. In general one can only define them implicitly involving Stieltjes transform or obtain by direct numerical simulation. Another simpler approximation investigated in Ref. [8] is when the parameter matrix Σ is a scalar times an identity matrix, that is $\Sigma = \alpha I_n$. For this simplified case the density of the eigenvalues can be given the MP density (38). The constants appearing in this equation can be obtained from Eqs. (41) and (42). In Fig. 1 the density of first 40 and 600 eigenvalues of the deterministic system is compared with the MP density (38). The histograms are computed from the eigenvalues obtained using the finite element method. The MATLABTM function `ksdensity` is used to obtain the density (the dashed line). It can be seen that the simple MP density function agrees reasonably well with the Finite Element results. Clearly with 40 eigenvalues the density is not very accurate, as can be seen from the histogram in Fig. 1(a). When large number of eigenvalues are used, as in Fig. 1(b), the pattern of the density function becomes obvious from the histogram. For this particular simple example of a plate, this can also be explained using analytical expressions.

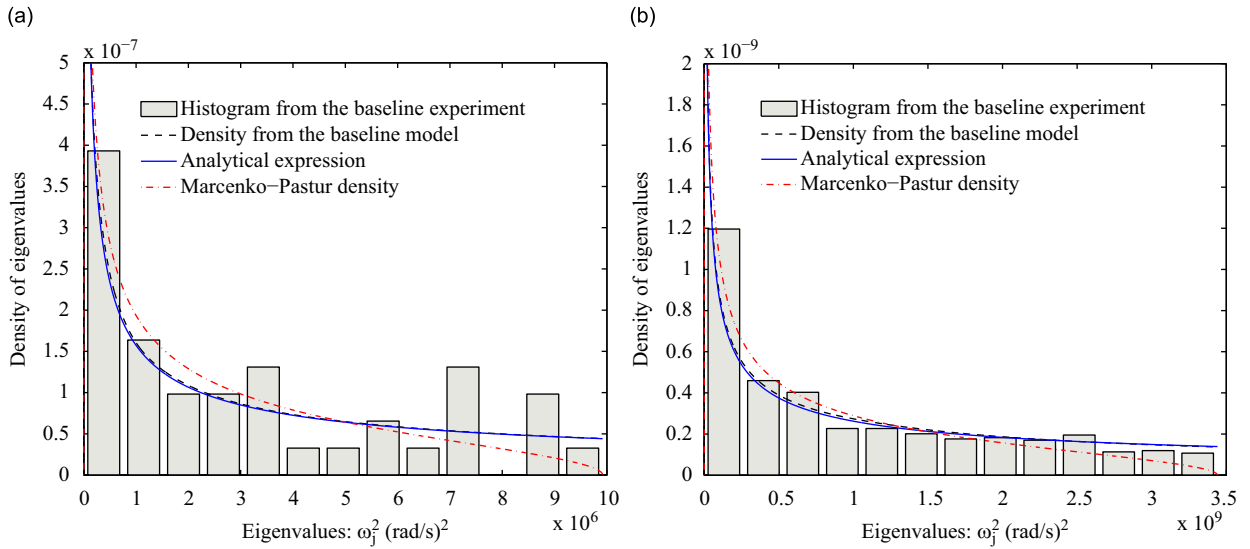


Fig. 1. The density of eigenvalues of the baseline plate model. (a) Density of the first 40 eigenvalues, (b) density of the first 600 eigenvalues.

The (non-normalized) density of the natural frequencies (square root of the eigenvalues) of a plate can be obtained using the analytical expression derived by Xie et al. [52] as

$$v(\omega) = \frac{L_x k_y}{4\pi} \sqrt{\frac{m t_h}{D}} + \frac{1}{2} \left(\frac{\rho t_h}{D} \right)^{1/4} \left(\frac{L_x + k_y}{\pi} \right) \omega^{-1/2}, \tag{43}$$

where $D = E t_h^3 / (12(1 - \mu^2))$. The quantity $v(\omega)$ is also known as the modal density. The constant modal density for plates, often assumed in many approximate methods for high-frequency vibration analysis, only arises when frequency is high enough so that only the first term dominates in Eq. (43). To convert Eq. (43) to a probability density function comparable to those shown in Fig. 1, we have to (a) first perform a change of variable $\lambda = \omega^2$, and (b) normalize the resulting function so that the total area under the curve is unity. Considering the transformation $\lambda = \omega^2$ and noting that we are interested only in the positive values, one can derive (see for example [53])

$$\rho(\lambda) = \frac{1}{c_p} \frac{v(\sqrt{\lambda})}{\sqrt{\lambda}}, \tag{44}$$

here c_p , the normalization constant, is derived such that the expression (44) results into unity when integrated between λ_{\min} and λ_{\max} . We can show that

$$\rho(\lambda) = \frac{1}{c_p} \left\{ \frac{L_x k_y}{4\pi} \sqrt{\frac{m t_h}{D}} \lambda^{-1/2} + \frac{1}{2} \left(\frac{\rho t_h}{D} \right)^{1/4} \left(\frac{L_x + k_y}{\pi} \right) \lambda^{-3/4} \right\}, \tag{45}$$

where

$$c_p = \frac{L_x k_y}{2\pi} \sqrt{\frac{m t_h}{D}} (\lambda_{\max}^{1/2} - \lambda_{\min}^{1/2}) + 2 \left(\frac{\rho t_h}{D} \right)^{1/4} \left(\frac{L_x + k_y}{\pi} \right) (\lambda_{\max}^{1/4} - \lambda_{\min}^{1/4}). \tag{46}$$

Eq. (45) is plotted in Fig. 1 by a solid line. Observe that the density obtained using all the approaches match well. The results in Fig. 1 show that Wishart random matrix model can be used even in the lower frequency range where the modal density is not constant.

From the numerical results we observe that a simple Wishart random matrix model leading to the MP density (38) is not a very bad approximation when compared to exact analytical expression. However that unlike Eq. (45), which is only applicable to a rectangular plate, the MP density (38) is applicable to a general positive definite system. It only uses the information regarding the minimum and maximum of the eigenvalues. We refer the readers to the book by Tulino and Verdú [23] for further discussion on the generality of the MP density.

Two different cases of uncertainties are considered next. In the first case it is assumed that the material properties are randomly inhomogeneous. In the second case we consider that the plate is ‘perturbed’ by attaching spring–mass oscillators at random locations. The stochastic finite element method is used for the first case, while experimental method is used for the second case.

4.1. Plate with randomly inhomogeneous material properties

It is assumed that the Young’s modulus, Poisson’s ratio, mass density and thickness are random fields of the form

$$E(\mathbf{x}) = \bar{E}(1 + \epsilon_E f_1(\mathbf{x})), \quad \mu(\mathbf{x}) = \bar{\mu}(1 + \epsilon_\mu f_2(\mathbf{x})), \tag{47}$$

$$m(\mathbf{x}) = \bar{m}(1 + \epsilon_m f_3(\mathbf{x})) \quad \text{and} \quad t(\mathbf{x}) = \bar{t}(1 + \epsilon_t f_4(\mathbf{x})). \tag{48}$$

The two dimensional vector \mathbf{x} denotes the spatial coordinates. The strength parameters are assumed to be $\epsilon_E = 0.10$, $\epsilon_\mu = 0.10$, $\epsilon_m = 0.08$ and $\epsilon_t = 0.12$. The random fields $f_i(\mathbf{x})$, $i = 1, \dots, 4$ are assumed to be correlated homogeneous Gaussian random fields. The autocorrelation function of each random fields in each direction is assumed to be an exponentially decaying function

$$C_{f_i}(x_1, x_2) = e^{-(|x_1 - x_2|)/\mu_{x_i}}. \tag{49}$$

It is assumed that the correlation length μ_{x_i} is 0.2 times the lengths in each direction. The exponential decay in the correlation function in Eq. (49) arises from the practical fact that the statistical correlation in the value of a particular property is expected to decrease the further the points become. The random fields are simulated by using the Karhunen–Loève expansion [1,53] involving uncorrelated standard normal variables. A 5000-sample Monte Carlo simulation is performed to obtain the eigenvalues of the system. The quantities $E(\mathbf{x})$, $\rho(\mathbf{x})$ and $t(\mathbf{x})$ are positive while $-1 \leq \nu(\mathbf{x}) \leq 1/2$ for all \mathbf{x} . Due to the bounded nature of these quantities, the Gaussian random field is not an ideal model for these quantities. However, due to small variability considered for these parameters, the probability that any of these quantities become non-physical is small. We have explicitly verified that all the realizations of these four random fields are physical in nature in our Monte Carlo simulation. In Fig. 2, 100 samples of the

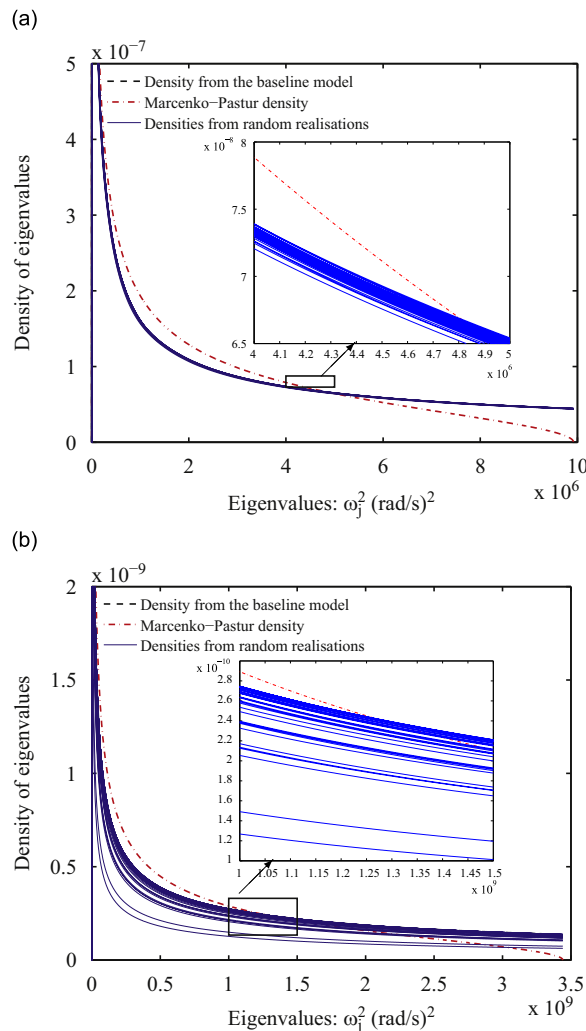


Fig. 2. The density of eigenvalues of the plate with randomly inhomogeneous material properties. The zoomed sections show the proximity of the eigenvalue-density of the random system. These results verify the self-averaging property of the eigenvalue density of a random system and the MP density. (a) Density of the first 40 eigenvalues, (b) density of the first 600 eigenvalues.

density of first 40 and 600 eigenvalues are shown, alongside the fitted MP density and density obtained from the baseline model. The numerical results shown here confirm theoretical results derived in the previous section. A small part of the density corresponding to the random samples have been zoomed for illustration. The proximity of the curves arising from the random sample corresponds to the self-averaging property proved in Section 3.2. Recall that the variance of the density of the eigenvalues around the mean decays in $O(n^{-2})$. We observe that the self-averaging property manifests itself even for 40 eigenvalues. The validity of the simple MP density (38) is also confirmed by Fig. 2. We can observe that for the bulk of the spectrum, the densities of the random system are fairly close to the MP density. From these results we conclude that MP density can represent the eigenvalue density of stochastically perturbed dynamical system considered here. Next we investigate this using an experimental study.

4.2. Plate with randomly attached spring–mass oscillators: experimental study

We consider the dynamics of a steel cantilever plate with homogeneous geometric (i.e., uniform thickness) and constitutive properties (i.e., uniform Young’s modulus and Poisson’s ratio) described in the previous section. This uniform plate defines (as considered in the numerical studies in the previous section) the baseline system. The baseline model is perturbed by a set of spring–mass oscillators with different natural frequencies and attached randomly along the plate. The details of this experiment have been described in [54]. Here we give a very brief overview. The overall arrangement of the test-rig is shown in Fig. 3(a).

The plate is clamped along one edge using a clamping device. The clamping device is attached on the top of a heavy concrete block and the whole assembly is placed on a steel table. The plate weights about 12.28 kg and special care has been taken to ensure its stability and minimizing the vibration transmission. In total 10 oscillators are used to simulate uncertainty in the system. The spring is glue-welded with a magnet at the top and a mass at the bottom. The magnet at the top of the assembly helps to attach the oscillators at the bottom of the plate repeatedly without much difficulty. The stiffness of the 10 springs used in the experiment are 16.800, 09.100, 17.030, 24.000, 15.670, 22.880, 17.030, 22.880, 21.360 and 19.800 kN/m. The oscillating mass of each of the 10 oscillators is 121.4 g. Therefore the total oscillating mass is 1.214 kg, which is 9.8 percent of the mass of the plate. The natural frequencies of the 10 oscillators are obtained as 59.2060, 43.5744, 59.6099, 70.7647, 57.1801, 69.0938, 59.6099, 69.0938, 66.7592 and 64.2752 Hz. The springs are attached to the plate at the pre-generated nodal locations using the small magnets located at the top of the assembly. The small magnets (weighting 2 g) are found to be strong enough to hold the 121.4 g mass attached to the spring below over the frequency range considered. One hundred realizations of the oscillators are created (by hanging the oscillators at random locations) and tested individually in this experiment. A 32 channel LMS™ [55] system and a shaker is employed to perform the modal analysis [56–58]. We used the shaker to act as an impulse hammer. The shaker was driven by a signal from a Simulink™ and dSpace™ system via a power amplifier. It generated impulses at a pulse rate of 20 s and a pulse width of 0.01 s. As seen in Fig. 3(a), 6 accelerometers are used as the response sensors. The signal from the force transducer is amplified using an amplifier while the signals from the accelerometers are directly input into the LMS system. For the data acquisition and processing, LMS Test Lab 5.0 is used. In the Impact Scope, we have set the bandwidth to 8192 Hz with 8192 spectral lines (i.e., 1.00 Hz resolution). Five averages are taken for each frequency response function (FRF) measurement. The amplitude of the driving-point FRF of the baseline system, FRFs corresponding to 100 realizations of the random system and the mean FRF amplitude is shown in Fig. 3(b).

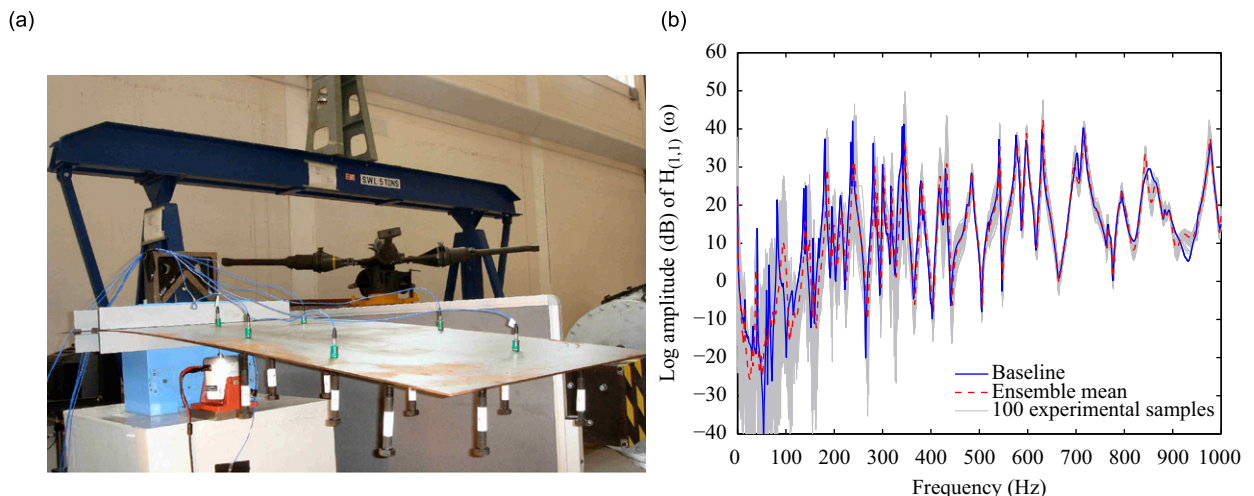


Fig. 3. The test rig and the measured frequency response functions (FRFs) of the cantilever plate driven by impulse. (a) Arrangement of the test-rig showing the plate and one realization of randomly placed oscillators, (b) experimentally measured driving point FRF of the baseline and 100 random systems.

The natural frequencies have been extracted [36] from the baseline FRF and each of the 100 measured FRFs shown in Fig. 3(b). The FRF corresponding to the bare plate (the baseline model) and the ensemble mean obtained from the 100 measured FRF are also shown in the paper. However, in this paper we do not consider the problem of calculating FRF statistics from the density of the eigenvalues. Every attempt was made to minimize damping in the plate during the experiment. It allowed us to reliably extract [36] upto first 40 natural frequencies of the baseline model as well as all the 100 random realizations.

The density of the first 40 eigenvalues (natural frequency squared) of the baseline model is shown in Fig. 4(a). Note that the experiential density matches perfectly with the analytical expression (45) derived before. This in turn validates the numerical model used in the previous section. In Fig. 4(b), the eigenvalue densities obtained from 100 experiments simulating the random system are shown. A small part of the density curves corresponding to the random samples have been zoomed for illustration. The proximity of the curves arising from the experiential samples verifies the self-averaging property proved in Section 3.2. We observe that the self-averaging property is acceptable even for 40 experimentally extracted eigenvalues. The validity of MP density (38) is also examined in Fig. 4(b). We observe that experimental densities of the random system are close to the MP density. From these results we conclude that MP density can represent the eigenvalue density for the experiential case study considered here. Next we consider numerical example of a complex system to further investigate the generality of these conclusions.

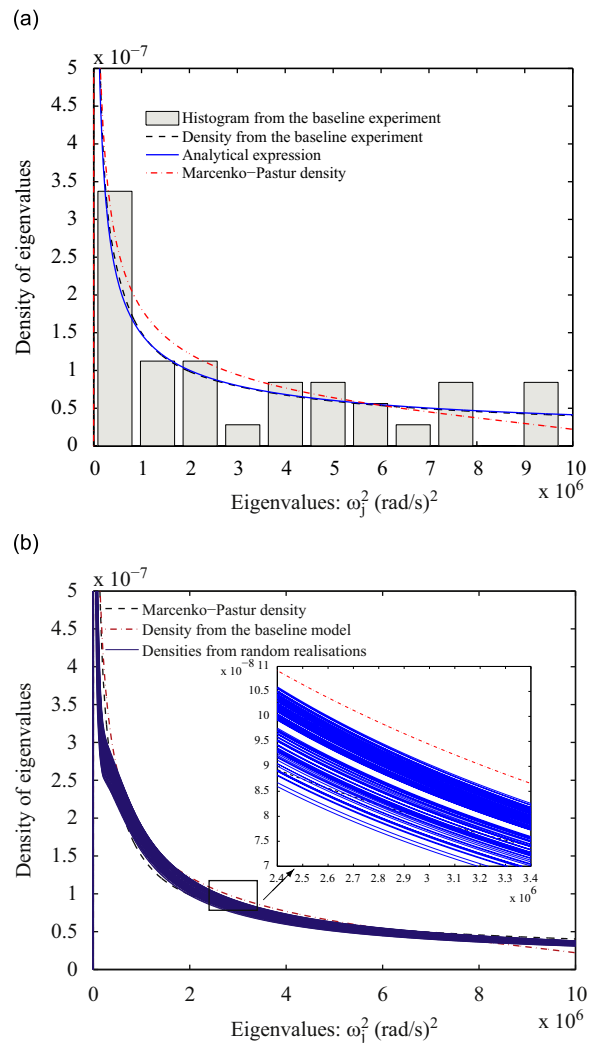


Fig. 4. The density of eigenvalues of the cantilevered plate with randomly attached oscillators obtained from the experiment. The zoomed section in (b) shows the proximity of all 100 eigenvalue-density obtained for the random system. These results experimentally validate the self-averaging property of the eigenvalue density of a random system and the MP density. (a) Density of the first 40 eigenvalues of the baseline system, (b) density of the first 40 eigenvalues of 100 random realizations.

5. Numerical study of a complex system: a helicopter tail boom

To investigate the generality of the results derived in this paper, we consider the tail boom of a Lynx helicopter. A finite element model of the tail boom is created, consisting of 1142 beam elements and 2373 shell elements. Detailed models of the tail rotor and gearboxes are not available but these components are included as point masses, with rigid constraints to distribute the inertial loads. The resultant model is comprised of 2186 nodes, corresponding to 13,116 DOFs.

The tail boom model is then constrained at the root, using rigid constraints between the tail boom attachment points and a single central node, and applying the absolute constraint at the central node. Eight regions are chosen for parametrisation, seven of which are depicted in Fig. 5. They broadly cover: the top and bottom of the main tail cone; the back, right and left sides of the tail fin; and the tailplane, comprised of two distinct regions, one covering most of the tailplane and one small reinforced section. The final region chosen for parametrisation is a bulkhead located midway along the tail cone. The shells from these eight regions are subject to thickness variations, with standard deviations ranging between seven percent and nine percent of the nominal deterministic values, as listed in Table 1. The vast majority of the structure is aluminium, with a density of 3728 kg/m^3 and Young's modulus of 72 GPa.

A Monte Carlo simulation is performed and the first 100 eigenvalues are calculated for each sample. Fig. 6 shows 150 samples of the eigenvalue densities from the Monte Carlo results alongside the density curve from the baseline model. The first 40 and 100 eigenvalues are considered for illustration. The fitted MP density is also plotted. Again a small part of the density corresponding to the random samples has been zoomed for illustration for both cases. The proximity of the curves arising from the random samples verifies the self-averaging property in Eq. (22). The validity of the simple MP density (38) is also verified in Fig. 6. We observe that the MP density is not as close as in the previous examples, although the general trend is similar.

Numerical results obtained in this paper show that the density of eigenvalues effectively 'converges' to a non-random quantity for a random dynamical system when the dimension of the system n is sufficiently large. When finite element modeling used, the dimension n is also related to the discretization of underlying continuum boundary value problem. The convergence of the numerical values of the finite element results with respect to n is a very different topic compared to the 'convergence' of the density of the eigenvalues discussed here. Eq. (22) states that the variance of the density of the eigenvalues about the mean density vanishes for large n . The variance given by (22) is the property of the underlying

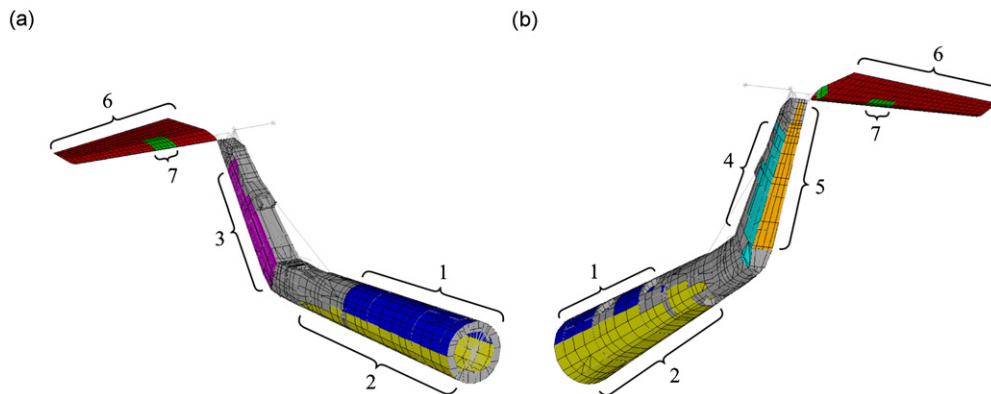


Fig. 5. The finite element model of the Lynx tail boom, showing the regions used for parametrisation. The model consists of 1142 beam elements, 2373 shell elements, 2186 nodes and 13,116 DOFs. (a) View from above, front, right, (b) view from below, back, left.

Table 1

Thickness variations of the eight regions in the Lynx tail boom for the Monte Carlo simulation.

Label (as used in Fig. 5)	Description	Mean thickness (mm)	Standard deviation (mm)
1	Cone: top	1.6	0.128
2	Cone: bottom	1.8	0.162
3	Fin: right	1.0	0.080
4	Fin: left	1.0	0.070
5	Fin: back	1.0	0.090
6	Tailplane: main	1.0	0.070
7	Tailplane: reinforced section	2.0	0.160
8	Mid-section bulkhead	1.4	0.098

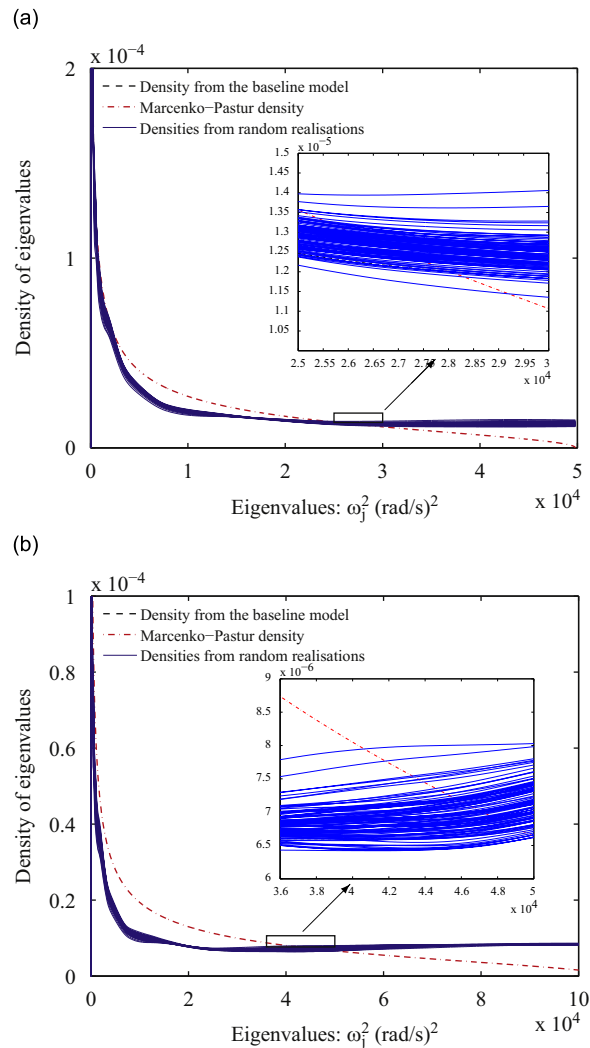


Fig. 6. The density of eigenvalues of the Lynx tail boom with random shell thickness variations (the model has 13,116 DOFs). The zoomed sections show the proximity of the eigenvalue-density of the random system. These results verify the self-averaging property of the eigenvalue density of a random system. (a) Density of the first 40 eigenvalues, (b) density of the first 100 eigenvalues.

random ensemble of dimension n , whereas the convergence of the numerical results of a finite element model is related to a *particular system realization* of dimension n .

6. Conclusions

The density of eigenvalues of linear structural dynamical systems with uncertainty is considered. Due to the positive definiteness nature of a real system, a Wishart random matrix model is considered. The parameters of the Wishart matrix are explicitly obtained from the baseline model and the dispersion parameters corresponding to the mass and stiffness matrices of the system. The main contributions of the paper are the following:

1. For large random systems, the density of eigenvalues reaches a non-random limit (the self-averaging property). In particular, it was rigorously proved that for a n -dimensional system, the variance associated with a linear statistic of the eigenvalues is in the order $O(n^{-2})$. Mathematically this is similar to the law of large numbers in the probability theory which says that the density of the sum of a large number of i.i.d. random variables is independent of the distribution of the random variables.
2. The eigenvalue density of a random dynamical system can be obtained from the eigenvalue density of the baseline model using an expression involving the Stieltjes transform of certain functionals.

3. Under certain restrictive assumptions, the Stieltjes transform expression can be simplified and the density of the eigenvalues can be represented by a closed-form expression known as the MP density function. This is a simple expression and all its parameters have been explicitly derived.

These results have been validated using limited number of numerical and experimental studies. Two numerical examples involving a cantilever plate (4650 DOF) with parametric uncertainty modeled by random fields and a helicopter tail boom (13,116 DOF) with parametric uncertainty modeled by random variables have been used to investigate the validity of the theoretical results. Using direct Monte Carlo simulations, it was indeed observed that eigenvalue-densities of nominally identical systems are close to each other. It was shown that the MP density is a reasonable approximation to the eigenvalue density function of the random systems considered.

The validity of the results derived in the paper has also been investigated using experimental data. Random eigenvalues in a vibrating plate due to disorderly attached spring-mass oscillators with random natural frequencies are considered. One hundred nominally identical dynamical systems were physically generated and individually tested in a laboratory setup. From the measured frequency response functions, 40 natural frequencies have been extracted for each of the 100 realizations. Eigenvalue densities were calculated for all 100 realizations and their proximity was observed. Like the numerical results, the MP density provides a reasonable approximation to the density function.

Acknowledgements

SA acknowledges the support of Royal Society through the award of Wolfson Research Merit award.

Appendix A. The details of the mathematical derivations in Section 3

We outline here the derivation of expressions (19) and (32). For technical simplicity we consider the hermitian analog of the Wishart matrices, called often the Laguerre Ensemble. The result for the real symmetric, i.e., genuine Wishart matrices (27), can be obtained analogously. Consider random matrices (cf. (27)) of the form

$$\Xi = p^{-1} \Sigma^{1/2} \mathbf{X} \mathbf{X}^* \Sigma^{1/2}, \tag{A.1}$$

where Σ is an $n \times n$ hermitian positive definite matrix, $\mathbf{X} = \{X_{j\alpha}\}_{j,\alpha=1}^{n,p}$ is the $n \times p$ matrix, whose entries are the standard complex Gaussian random variables, i.e.,

$$\mathbb{E}\{X_{j\alpha}\} = \mathbb{E}\{X_{j_1\alpha_1} X_{j_2\alpha_2}\} = 0, \quad \mathbb{E}\{X_{j_1\alpha_1} \overline{X_{j_2\alpha_2}}\} = \delta_{j_1 j_2} \delta_{\alpha_1 \alpha_2}, \tag{A.2}$$

$\overline{X_{j\alpha}}$ is the complex conjugate of $X_{j\alpha}$, and \mathbf{X}^* is the hermitian conjugate of \mathbf{X} .

Proof of (19) for $\beta = 2$. The proof can be given by following the steps:

(i) Given the standard complex Gaussian random variables $\{\zeta_l\}_{l=1}^q$

$$\mathbb{E}\{\zeta_l\} = \mathbb{E}\{\zeta_l \zeta_m\} = 0, \quad \mathbb{E}\{\zeta_l \overline{\zeta_m}\} = \delta_{lm} \tag{A.3}$$

and a differentiable function Φ of $2q$ complex variables, consider the random variable

$$\Psi = \Phi(\zeta_1, \dots, \zeta_q, \overline{\zeta_1}, \dots, \overline{\zeta_q}).$$

Then its variance admits the bound

$$\mathbb{V}\{\Psi\} := \mathbb{E}\{|\Psi|^2\} - |\mathbb{E}\{\Psi\}|^2 \leq \sum_{l=1}^q \mathbb{E} \left\{ \left| \frac{\partial \Phi}{\partial \zeta_l} \right|^2 + \left| \frac{\partial \Phi}{\partial \overline{\zeta}_l} \right|^2 \right\}, \tag{A.4}$$

known as the Poincaré inequality (see e.g. [59]).

(ii) Given hermitian matrix $\mathbf{A}(t)$ depending on a parameter t and a function $\varphi : \mathbb{R} \rightarrow \mathbb{C}$, consider the matrix function $\varphi(\mathbf{A}(t))$. Then we have

$$\frac{d}{dt} \text{Tr} \varphi(\mathbf{A}(t)) = \text{Tr} \varphi'(\mathbf{A}(t)) \mathbf{A}'(t). \tag{A.5}$$

It follows from (A.1) that the entries $\{\Xi_{jk}\}_{j,k=1}^n$ of Ξ are

$$\Xi_{jk} = p^{-1} \sum_{l,m=1}^n \sum_{\alpha=1}^p R_{jl} X_{l\alpha} \overline{X_{m\alpha}} R_{mk}, \tag{A.6}$$

where $\mathbf{R} = \Sigma^{1/2}$. Besides, it follows from the spectral theorem for hermitian matrices and (16) that

$$N_n[\varphi] = n^{-1} \text{Tr} \varphi(\Xi).$$

Take in (A.4) $n^{-1} \text{Tr } \varphi(\Xi)$ as Ψ and $\{X_{\alpha j}\}_{\alpha,j=1}^{p,n}$ as $\{\zeta_l\}_{l=1}^q$, hence, $q=np$. This yields

$$\mathbb{V}\{N_n[\varphi]\} \leq n^{-2} \sum_{\alpha=1}^p \sum_{j=1}^n \mathbb{E} \left\{ \left| \frac{\partial \text{Tr } \varphi(\Xi)}{\partial X_{j\alpha}} \right|^2 + \left| \frac{\partial \text{Tr } \varphi(\Xi)}{\partial \bar{X}_{j\alpha}} \right|^2 \right\}. \tag{A.7}$$

Take now in (A.5) $X_{j\alpha}$ as t , $p^{-1} \mathbf{RXX}^* \mathbf{R}$ as \mathbf{A} and use the formulas (see (A.6))

$$\frac{\partial}{\partial X_{j\alpha}} (\mathbf{RXX}^* \mathbf{R})_{lm} = R_{ij} (\mathbf{X}^* \mathbf{R})_{\alpha m}, \quad \frac{\partial}{\partial \bar{X}_{j\alpha}} (\mathbf{RXX}^* \mathbf{R})_{lm} = R_{jm} (\mathbf{R}\mathbf{X})_{l\alpha}. \tag{A.8}$$

This yields after a simple algebraic manipulation

$$\mathbb{V}\{N_n[\varphi]\} \leq \frac{2}{n^2 p} \mathbb{E}\{\text{Tr } \Xi \varphi'(\Xi) \Sigma \bar{\varphi}'(\Xi)\} = \frac{2}{n^2 p} \mathbb{E}\{\text{Tr } \bar{\varphi}'(\Xi) \varphi'(\Xi) \Sigma^{1/2} \Xi \Sigma^{1/2}\}.$$

(iii) Now we use the inequality $|\text{Tr } \mathbf{A}\mathbf{B}| \leq \|\mathbf{A}\| \text{Tr } \mathbf{B}$, valid for any matrix \mathbf{A} ($\|\mathbf{A}\|$ is the Euclidian norm of \mathbf{A}) and a positive definite \mathbf{B} . Choosing $A = \bar{\varphi}'(\Xi) \varphi'(\Xi)$ and $B = \Sigma^{1/2} \Xi \Sigma^{1/2}$ we obtain

$$|\text{Tr } \Xi \varphi'(\Xi) \Sigma \bar{\varphi}'(\Xi)| \leq \|\varphi'(\Xi)\|^2 \text{Tr } \Xi \Sigma.$$

(iv) The inequality $\|\psi(\Xi)\| \leq \max_{x \in \mathbb{R}} |\psi(x)|$, valid a hermitian Ξ and any function ψ and implying that

$$\mathbb{V}\{N_n[\varphi]\} \leq \frac{2}{n^2 p} \left(\max_{x \in \mathbb{R}} |\varphi'(x)| \right)^2 \mathbb{E}\{\text{Tr } \Xi \Sigma\}. \tag{A.9}$$

It follows now from (A.2) that

$$\mathbb{E}\{\text{Tr } \Xi \Sigma\} = \text{Tr } \Sigma^2.$$

Plugging this in (A.9) and using (20), we obtain (19) with $\beta = 2$. The case $\beta = 1$ is similar. \square

Proof of (29)–(38). Let N_n be the Normalized Counting measure of eigenvalues $\{\lambda_l^{(n)}\}_{l=1}^n$, defined for any interval Δ of spectral axis as

$$N_n(\Delta) = \#\{l = 1, \dots, n : \lambda_l^{(n)} \in \Delta\} / n. \tag{A.10}$$

The measure N_n has ρ_n of (11) as its density. It follows from the spectral theorem for hermitian matrices that the Stieltjes transform of N_n is

$$g_n(z) := \int \frac{dN_n(\lambda)}{\lambda - z} = \frac{1}{n} \sum_{l=1}^n \frac{1}{\lambda_l^{(n)} - z} = \frac{1}{n} \text{Tr}(\Xi - z\mathbf{I}_n)^{-1}, \quad \Im z \neq 0.$$

Our goal is to prove that the limit

$$f(z) := \lim_{p,n \rightarrow \infty, p/n \rightarrow c \in [1, \infty)} \mathbb{E}\{g_n(z)\}$$

satisfies (32). Indeed, this and the general properties of the Stieltjes transform (see e.g. [60], Section 59) imply (29) and (38).

By using the identity

$$(\mathbf{A} - z\mathbf{I}_n)^{-1} = -z^{-1} + z^{-1}(\mathbf{A} - z\mathbf{I}_n)^{-1}$$

and (A.1), we write

$$\begin{aligned} f_n(z) &:= \mathbb{E}\{g_n(z)\} = -z^{-1} + (nz)^{-1} \mathbb{E}\{\text{Tr } \Xi(\Xi - z\mathbf{I}_n)^{-1}\} = -z^{-1} + (pnz)^{-1} \mathbb{E}\{\text{Tr } \mathbf{X}^* \Sigma \mathbf{X}(p^{-1} \mathbf{X}^* \Sigma \mathbf{X} - z\mathbf{I}_n)^{-1}\} \\ &= -z^{-1} + (nz)^{-1} \mathbb{E}\{\text{Tr } \mathbf{K}\}, \end{aligned} \tag{A.11}$$

where we used the cyclicity of trace ($\text{Tr } \mathbf{ABC} = \text{Tr } \mathbf{BCA}$) and denoted

$$\mathbf{Q} = p^{-1} \Sigma \mathbf{X} \mathbf{G} \mathbf{X}^*, \quad \mathbf{G} = (p^{-1} \mathbf{X}^* \Sigma \mathbf{X} - z\mathbf{I}_n)^{-1}. \tag{A.12}$$

We need now the formula, valid for the standard Gaussian complex variables $(\zeta_1, \dots, \zeta_q, \bar{\zeta}_1, \dots, \bar{\zeta}_q)$

$$\mathbb{E}\{\zeta_l \Phi(\zeta_1, \dots, \zeta_q, \bar{\zeta}_1, \dots, \bar{\zeta}_q)\} = \mathbb{E}\left\{ \frac{\partial}{\partial \bar{\zeta}_l} \Phi(\zeta_1, \dots, \zeta_q, \bar{\zeta}_1, \dots, \bar{\zeta}_q) \right\}, \tag{A.13}$$

which can be proved by integration by parts, and the formula (A.8)

$$\frac{\partial G_{\alpha\beta}}{\partial X_{l\alpha}} = p^{-1} G_{\alpha\alpha} (\Sigma \mathbf{X} \mathbf{G})_{l\beta}$$

for \mathbf{G} of (A.12), which follows from the first-order perturbation formula

$$\delta \mathbf{G} = p^{-1} \mathbf{G} \delta \mathbf{X}^* \mathbf{X} \mathbf{G} + O((\delta \mathbf{X}^*)^2)$$

and (A.8) (note that we treat \mathbf{X} and \mathbf{X}^* as independent quantities, according to (A.2) and (A.13)).

Now, writing

$$\mathbb{E}\{Q_{jk}\} = p^{-1} \sum_{\alpha, \beta=1}^p \sum_{l=1}^n \mathbb{E}\{\Sigma_{jl} X_{l\alpha} G_{\alpha\beta} \overline{X_{k\beta}}\}$$

and taking $X_{l\alpha}$ as ζ_l and $G_{\alpha\beta} \overline{X_{k\beta}}$ as Φ in (A.13), we obtain the matrix relation

$$\mathbb{E}\{\mathbf{Q}\} = h_n(z) \mathbf{\Sigma} - h_n(z) \mathbf{\Sigma} \mathbb{E}\{\mathbf{Q}\} - \mathbf{\Sigma} \mathbb{E}\{\overset{\circ}{S}_n(z) \mathbf{Q}\},$$

where

$$s_n(z) = p^{-1} \text{Tr } \mathbf{G}, \quad h_n(z) = \mathbb{E}\{s_n(z)\}, \quad \overset{\circ}{s}_n(z) = s_n(z) - h_n(z).$$

The relation implies

$$\mathbb{E}\{\mathbf{Q}\} = h_n(z) \mathbf{\Sigma} (1 + h_n(z) \mathbf{\Sigma})^{-1} - \mathbf{\Sigma} (1 + h_n(z) \mathbf{\Sigma})^{-1} \mathbb{E}\{\overset{\circ}{S}_n(z) \mathbf{Q}\}. \tag{A.14}$$

Substituting this into (A.11), we obtain that

$$f_n(z) = -z^{-1} + (nz)^{-1} h_n(z) \text{Tr } \mathbf{\Sigma} (1 + h_n(z) \mathbf{\Sigma})^{-1} - z^{-1} \mathbb{E}\{\overset{\circ}{S}_n(z) n^{-1} \text{Tr } \mathbf{\Sigma} (1 + h_n(z) \mathbf{\Sigma})^{-1} \mathbf{Q}\}. \tag{A.15}$$

It follows from (19) with $\varphi(\lambda) = (\lambda - z)^{-1}$, $\Im z \neq 0$, that

$$\mathbb{V}\{s_n(z)\} := \mathbb{E}\{|\overset{\circ}{S}_n(z)|^2\} \leq \frac{2C}{pn |\Im z|^2},$$

where C is defined in (20).

This allows one to prove that the third term on the r.h.s. of (A.15) is $O(n^{-1})$ (even $O(n^{-2})$). This and the spectral theorem for the positive definite correlation matrix $\mathbf{\Sigma}$ yield

$$f_n(z) = -z^{-1} + (nz)^{-1} h_n(z) \sum \frac{\sigma_l}{1 + h_n(z) \sigma_l} + O(n^{-1}),$$

where $\{\sigma_l\}_{l=1}^n$ are eigenvalues of $\mathbf{\Sigma}$. Thus, assuming that there exists the limiting distribution ν of σ 's, we obtain in the limit (18)

$$f(z) = -\frac{1}{z} + \frac{h(z)}{z} \int \frac{\sigma \nu(\sigma) d\sigma}{1 + h(z) \sigma}. \tag{A.16}$$

Note now that for $p \geq n$ the $p \times p$ matrix $\mathbf{X}^* \mathbf{\Sigma} \mathbf{X}$ has $p - n$ zero eigenvalues and the rest of them coincide with those of $\mathbf{\Sigma}^{1/2} \mathbf{X} \mathbf{X}^* \mathbf{\Sigma}^{1/2}$. This implies

$$h_n(z) = -\frac{1}{z} \frac{p-n}{p} + \frac{n}{p} f_n(z),$$

hence, the limiting relation

$$h(z) = -\frac{1}{z} \left(1 - \frac{1}{c}\right) + \frac{1}{c} f(z). \tag{A.17}$$

Now it is easy to find that (A.16) and (A.17) imply (32). \square

References

- [1] R. Ghanem, P. Spanos, *Stochastic Finite Elements: A Spectral Approach*, Springer-Verlag, New York, USA, 1991.
- [2] A. Haldar, S. Mahadevan, *Reliability Assessment Using Stochastic Finite Element Analysis*, John Wiley and Sons, New York, USA, 2000.
- [3] C. Soize, A nonparametric model of random uncertainties for reduced matrix models in structural dynamics, *Probabilistic Engineering Mechanics* 15 (3) (2000) 277–294.
- [4] C. Soize, Maximum entropy approach for modeling random uncertainties in transient elastodynamics, *Journal of the Acoustical Society of America* 109 (5) (2001) 1979–1996 (part 1).
- [5] M. Arnst, D. Clouteau, H. Chebli, R. Othman, G. Degrande, A non-parametric probabilistic model for ground-borne vibrations in buildings, *Probabilistic Engineering Mechanics* 21 (1) (2006) 18–34.
- [6] M.P. Mignolet, C. Soize, Nonparametric stochastic modeling of linear systems with prescribed variance of several natural frequencies, *Probabilistic Engineering Mechanics* 23 (2–3) (2008) 267–278.
- [7] S. Adhikari, Wishart random matrices in probabilistic structural mechanics, *ASCE Journal of Engineering Mechanics* 134 (12) (2008) 1029–1044.
- [8] S. Adhikari, Generalized Wishart distribution for probabilistic structural dynamics, *Computational Mechanics* 45 (5) (2010) 495–511.
- [9] H. Benaroya, M. Rehak, Finite element methods in probabilistic structural analysis: a selective review, *Applied Mechanics Reviews, ASME* 41 (5) (1988) 201–213.
- [10] H. Benaroya, Random eigenvalues, algebraic methods and structural dynamic models, *Applied Mathematics and Computation* 52 (1992) 37–66.
- [11] M. Grigoriu, A solution of random eigenvalue problem by crossing theory, *Journal of Sound and Vibration* 158 (1) (1992) 69–80.

- [12] C. Lee, R. Singh, Analysis of discrete vibratory systems with parameter uncertainties, part I: eigensolution, *Journal of Sound and Vibration* 174 (3) (1994) 379–394.
- [13] M. Hála, Method of Ritz for random eigenvalue problems, *Kybernetika* 30 (3) (1994) 263–269.
- [14] S. Mehlhose, J. vom Scheidt, R. Wunderlich, Random eigenvalue problems for bending vibrations of beams, *Zeitschrift Fur Angewandte Mathematik Und Mechanik* 79 (10) (1999) 693–702.
- [15] S. Adhikari, M.I. Friswell, Random matrix eigenvalue problems in structural dynamics, *International Journal for Numerical Methods in Engineering* 69 (3) (2007) 562–591.
- [16] D. Ghosh, R.G. Ghanem, J. Red-Horse, Analysis of eigenvalues and modal interaction of stochastic systems, *AIAA Journal* 43 (10) (2005) 2196–2201.
- [17] P.B. Nair, A.J. Keane, An approximate solution scheme for the algebraic random eigenvalue problem, *Journal of Sound and Vibration* 260 (1) (2003) 45–65.
- [18] C.V. Verhoosel, M.A. Gutiérrez, S.J. Hulshoff, Iterative solution of the random eigenvalue problem with application to spectral stochastic finite element systems, *International Journal for Numerical Methods in Engineering* 68 (4) (2006) 401–424.
- [19] S. Rahman, A solution of the random eigenvalue problem by a dimensional decomposition method, *International Journal for Numerical Methods in Engineering* 67 (9) (2006) 1318–1340.
- [20] J. Wishart, The generalized product moment distribution in samples from a normal multivariate population, *Biometrika* 20 (A) (1928) 32–52.
- [21] E.P. Wigner, On the distribution of the roots of certain symmetric matrices, *Annals of Mathematics* 67 (2) (1958) 325–327.
- [22] F. Mezzadri, N.C. Snaith (Eds.), *Recent Perspectives in Random Matrix Theory and Number Theory*, London Mathematical Society Lecture Note, Cambridge University Press, Cambridge, UK, 2005.
- [23] A.M. Tulino, S. Verdú, *Random Matrix Theory and Wireless Communications*, now Publishers Inc., Hanover, MA, USA, 2004.
- [24] M.L. Eaton, *Multivariate Statistics: A Vector Space Approach*, John Wiley and Sons, New York, 1983.
- [25] V.L. Girko, *Theory of Random Determinants*, Kluwer Academic Publishers, The Netherlands, 1990.
- [26] R.J. Muirhead, *Aspects of Multivariate Statistical Theory*, John Wiley and Sons, New York, USA, 1982.
- [27] M.L. Mehta, *Random Matrices*, second ed., Academic Press, San Diego, CA, 1991.
- [28] L. Pastur, M. Shcherbina, *Eigenvalue Distribution of Large Random Matrices*, American Mathematical Society, Providence, RI, USA, 2011.
- [29] V. Girko, *Theory of Stochastic Canonical Equations*, vols. I and II, Kluwer, Dordrecht, 2001.
- [30] L. Pastur, *Random Matrices as Paradigm*, *Mathematical Physics 2000*, Imperial College Press, London, UK, 2000, pp. 216–266.
- [31] V.I. Serdobolskii, *Multiparametric Statistics*, Kluwer, Dordrecht, Netherlands, 2008.
- [32] O.C. Zienkiewicz, R.L. Taylor, *The Finite Element Method*, fourth ed., McGraw-Hill, London, 1991.
- [33] D. Dawe, *Matrix and Finite Element Displacement Analysis of Structures*, Oxford University Press, Oxford, UK, 1984.
- [34] K. Bathe, *Finite Element Procedures in Engineering Analysis*, Prentice-Hall Inc., New Jersey, 1982.
- [35] R.D. Cook, D.S. Malkus, M.E. Plesha, R.J. Witt, *Concepts and Applications of Finite Element Analysis*, fourth ed., John Wiley and Sons, New York, USA, 2001.
- [36] S. Adhikari, A.S. Phani, Random eigenvalue problems in structural dynamics: experimental investigations, *AIAA Journal* 48 (6) (2010) 1085–1097.
- [37] A. Gupta, D. Nagar, *Matrix Variate Distributions, Monographs & Surveys in Pure & Applied Mathematics*, Chapman & Hall/CRC, London, 2000.
- [38] Z. Bai, J.W. Silverstein, *Spectral Analysis of Large Dimensional Random Matrices*, Science Press, Beijing, China, 2006.
- [39] J.L. du Bois, S. Adhikari, N.A.J. Lieven, On the quantification of eigenvalue curve veering: a veering index, *Transactions of ASME, Journal of Applied Mechanics* 78 (4) (2011) 041007:1–041007:8.
- [40] J.L. du Bois, S. Adhikari, N.A.J. Lieven, Mode veering in stressed framed structures, *Journal of Sound and Vibration* 322 (4–5) (2009) 1117–1124.
- [41] C.S. Manohar, A.J. Keane, Statistics of energy flow in one dimensional subsystems, *Philosophical Transactions of Royal Society of London A* 346 (1994) 525–542.
- [42] C. Soize, Random matrix theory and non-parametric model of random uncertainties in vibration analysis, *Journal of Sound and Vibration* 263 (4) (2003) 893–916.
- [43] S. Adhikari, Rates of change of eigenvalues and eigenvectors in damped dynamic systems, *AIAA Journal* 37 (11) (1999) 1452–1458.
- [44] S. Adhikari, Calculation of derivative of complex modes using classical normal modes, *Computer and Structures* 77 (6) (2000) 625–633.
- [45] F. Fahy, Statistical energy analysis—a critical overview, *Philosophical Transactions of the Royal Society of London, Series A—Mathematical Physical and Engineering Sciences* 346 (1681) (1994) 431–447.
- [46] O. Lobkis, R. Weaver, I. Rozhkov, Power variances and decay curvature in a reverberant system, *Journal of Sound and Vibration* 237 (2) (2000) 281–302.
- [47] R.S. Langley, A.W.M. Brown, The ensemble statistics of the energy of a random system subjected to harmonic excitation, *Journal of Sound and Vibration* 275 (2004) 823–846.
- [48] I.M. Lifshitz, S.A. Gredeskul, L.A. Pastur, *Introduction to the Theory of Disordered Systems*, Wiley, NY, USA, 1988.
- [49] A. Figotin, L. Pastur, *Spectra of Random and Almost-Periodic Operators*, Springer-Verlag, Berlin, Germany, 1992.
- [50] V. Marčenko, L. Pastur, The eigenvalue distribution in some ensembles of random matrices, *Mathematics of the USSR Sbornik* 1 (1967) 457–483.
- [51] J.W. Silverstein, Z.D. Bai, On the empirical distribution of eigenvalues of a class of large-dimensional random matrices, *Journal of Multivariate Analysis* 54 (1995) 175–192.
- [52] G. Xie, D.J. Thompson, C.J.C. Jones, Mode count and modal density of structural systems: relationships with boundary conditions, *Journal of Sound and Vibration* 274 (2004) 621–651.
- [53] A. Papoulis, S.U. Pillai, *Probability, Random Variables and Stochastic Processes*, fourth ed., McGraw-Hill, Boston, USA, 2002.
- [54] S. Adhikari, M.I. Friswell, K. Lonkar, A. Sarkar, Experimental case studies for uncertainty quantification in structural dynamics, *Probabilistic Engineering Mechanics* 24 (4) (2009) 473–492.
- [55] LMS Test Lab Spectral Acquisition User Manual, Rev 5A, Interleuvenlaan 68, B-3001 Leuven, Belgium, 2004.
- [56] D.J. Ewins, *Modal Testing: Theory and Practice*, second ed., Research Studies Press, Baldock, England, 2000.
- [57] N.M.M. Maia, J.M.M. Silva, J.B. Roberts (series editor) (Eds.), *Theoretical and Experimental Modal Analysis, Engineering Dynamics Series*, Research Studies Press, Taunton, England, 1997.
- [58] J.M.M. Silva, N.M.M. Maia (Eds.), *Modal Analysis and Testing: Proceedings of the NATO Advanced Study Institute, NATO Science Series: E: Applied Science*, Sesimbra, Portugal, 1998.
- [59] V. Bogachev, *Gaussian Measures*, American Mathematical Society, Providence, USA, 1991.
- [60] N.I. Akhiezer, I.M. Glazman, *Theory of Linear Operators in Hilbert Space*, Dover, NY, USA, 1993.